Spatiotemporal Variations in Surface Velocity of the Gangotri Glacier, Garhwal Himalaya, India: Study using Synthetic Aperture Radar Data

S. P. Satyabala

SUPPLEMENTARY SECTION

Section S1, Tables S1-S3, Figures S1-S6

Section S1: ANALYSIS OF WINDOW SIZES

Typically, a range of window sizes and sampling intervals are tried to find the optimum size for a given study (e.g. Abe &Furuya (2015), Pritchard et al. (2004), Remko de Lange et al. (2007)). The window size must be large enough to encompass the expected displacement and size of trackable features on the glacier surface. Larger windows may cause smoothing of offsets and also some attenuation of any real variations in the velocity map. Very small windows may not capture the features being tracked and the velocities determined will be noisier and have smaller SNR. Misregistrations or spurious data points can occur for window sizes that are too small so the features are not being tracked or too large so that so that the (zero) velocity of a non-moving portion of the image, e.g. on glacier margins, is assigned to a location on the glacier surface. Based on all these considerations, an optimum size is chosen such that the features being tracked are well represented and the velocity is not smoothed out: the size is optimised for maximum deformation signal with minimal noise.

Several window sizes have been tried and the best window size was determined for each satellite track used in this paper. In general, the smallerthe window size, the better the margins of the glacier are resolved, otherwise, the across profiles are unrealistically cropped at the glacier margins. But smaller windows result in more noisy offsets as the cross-correlation peaks become broader with increased window sizes and reduces the SNR value.

The results of offset-tracking for some window sizes (Table S3) are discussed here for the L-band ALOS PALSAR data. We present one summer and one winter offset-tracking pair to illustrate the impact of window size on our results. The center line (Figure S4) profiles of velocity along the glacier for these two window sizes are plotted in Figures S5A, for representative winter and summer pairs. It may be seen that profile for the largest window size (W0, used in all analysis of this paper) is smoother.

From Figure S5A for winter, we note that the smaller window sizes are more noisy but fluctuate around the smoother curve till ~20 km, beyond which the smaller windows give larger signal as well as larger SNR, indicating that the two are equivalent for obtaining the average velocity in the ablation region. This indicates that W0 gives the smoothest and best result for distances up to ~20 km but higher upglacier, the smaller window W3 seems better. These effects are possibly related to the features being tracked. In the ablation region, the features are more robust and also larger, hence the larger window size gives a better result while not obscuring the result. On the other hand, the effect on the accumulation region, where the trackable features are fewer and perhaps smaller, the smaller window sizes perform better with better SNR. The window size W3 seemed optimum for the accumulation region from ~20 upglacier, giving maximum deformation and also larger SNR. Hence, we presented the velocity map using W3 in Figure 3C for the region near the head of the glacier (H in Figure 2), where the velocity vectors are best resolved. Noisy correlations also generally cause noisy velocity vector directions (with no relation to the expected direction of movement along the glacier) and smaller SNR.

The winter velocities could be extracted almost along the entire length of the glacier while the summer velocities (Figure S5B) are noisy and are not resolvable beyond a distance ~12-15 km up-glacier from the terminus. It may be noted that SNR is smaller for the smaller window size and for summer pairs. The summer profiles are more noisy probably on account of changes on the glacier surface (between acquisition times of the two images) due to melting in the ablation region and/or snowfall further up-glacier which results in spurious correlations (unrealistic magnitude and/or direction of the velocity vector).

The profiles of velocity across the glacier at locations indicated in Figure S4 are shown in Figure S6. The profiles are truncated at the glacier margins beyond which the velocity vector directions deviate from the along-glacier azimuth. The summer profiles

appear truncated much before the glacier margins (marked by vertical thick black lines on the x-axis in each figure) for the bigger window size, while for the smaller window size these profiles continue nearly up to the glacier margin just as the winter profiles do. This truncation of the velocity profile at the margin of the glacier is physically unlikely and appears to be a localised artefact of window size chosen: When the portion of the glacier surface changes between acquisition times of the two images, the non-moving parts of the images just outside the glacier margins get over-represented in the offset-tracking procedure whereby the nearly zero velocity gets assigned to this particular pixel lying on the glacier surface. If the window size is smaller this effect is reduced and almost the entire width of the glacier has significant velocity.

It may be noted that this artefact of larger window sizes affects velocities only at the margins while the center-line velocity obtained is much more robust (for summer only up to ~15-20 km). Such artefacts have been noted by other workers e.g. Pritchard et al. (2004) who have attributed this to possible shearing/rotation locally of the glacier surface close to the margins. In our case, this artefact is likely due to change in surface features due to melting although shearing and/or rotation of the glacier surface near the margins cannot be ruled out. Evidence for surface changes due to melting on the Gangotri glacier is abundant in optical images acquired during summer months in the form of small melt-water ponds and melt-water streams in the ablation region and also to some extent further up-glacier. An additional factor, that may cause of surface change (and hence of this artefact in offset-tracking results) near the margins of the Gangotri glacier, could be avalanches that may have occurred between the acquisition of images forming the offset-tracking pair. Observations of avalanche events have been recorded and avalanche hazard zones have been identified nearly

all along the Gangotri glacier mostly on the eastern margin and to a lesser extent on the western margin (Snehmani et al. 2013).

Absence of this artefact for the winter profiles indicates that the surface features are more stable in winter as also indicated by the smoother profiles (along and across glacier) and the much larger SNR of the offset-tracking procedure.

Hence, all analysis for the data from PALSAR 521 was carried out using the window size W0 detailed in Table S3.

REFERENCES

Abe T. and M. Furuya (2015), Winter speed-up of quiescent surge-type glaciers in Yukon, Canada, *The Cryosphere*, 9, 1183–1190, 2015.

Bhambri, R. and T. Bolch., (2009) Glacier mapping: a review with special reference to the Indian Himalayas, Progress in Physical Geography, 33(5), 672–704.

Kääb Andreas, Etienne Berthier, Christopher Nuth, Julie Gardelle and Yves Arnaud (2012), Contrasting patterns of early twenty-first-century glacier mass change in the Himalayas, *Nature*, **488**, 495–498.

Kargel J.S., Cogley, J.G., Lenoard, G.J., Haritashya, U., Byers, A. (2011), Himalayan glaciers: The big picture is a montage, Proceedings of the National Academy of Sciences, 108 (36), 14709–14710

Kumar, K., R.K. Dumka, M.S. Miral, G.S. Satyal and M. Pant. (2008), Estimation of retreat rate of Gangotri glacier using rapid static and kinematic GPS survey, *Current Science*, **94**, 258-262.

Pritchard, H., T. Murray, A. Luckman, T. Strozzi, and S. Barr (2005), Glacier surge dynamics of Sortebræ, east Greenland, from synthetic aperture radar feature tracking, *Journal Geophysical Research*, **110**, F03005, doi:10.1029/2004JF000233.

Raina VK (2009), Himalayan Glaciers: A State-of-Art Review of Glacial Studies, Glacial Retreat and Climate Change, Discussion Paper (Ministry of Environment and Forests, Government of India, New Delhi).

Remko de Lange, R., Luckman, A., and Murray, T. (2007), Improvement of satellite radar feature tracking for ice velocity derivation by spatial frequency filtering, IEEE T. Geosci. Remote, 45, 2309–2318.

Rignot, E., Echelmeyer, K., &Krabill, W. (2001), Penetration depth of interferometric synthetic-aperture radar signals in snow and ice, *Geophysical Research Letters*, **28**(18), 3501–3504.

Scherler, D., B. Bookhagen, and M. R.Strecker (2011b), Hillslope-glacier coupling: The interplay of topography and glacial dynamics in High Asia, Journal Geophysical Research, 116, F02019, doi: 10.1029/2010JF001751.

Snehmani, A. Bhardwaj, A. Pandit and A. Ganju (2013), Demarcation of potential avalanche site using remote sensing and ground observations: a case study of Gangotri glacier, *Geocarto International*, DOI: 10.1080/10106049.2013.807304.

TABLES

Table S1: List of SAR images used

Sensor	Mode	Path (track)	Acquisition date	Ascending /Descending
ASAR	IS6	177	20101109	D
	IS6	177	20101209	D
	IS6	177	20110207	D
	IS6	177	20110309	D
	IS6	177	20110707	D
PALSAR	FBS	521	20070505	A
	FBD	521	20070805	A
	FBD	521	20070920	A
	FBS	521	20071105	A
	FBS	521	20080205	A
	FBS	521	20080322	A
	FBD	521	20080622	A
	FBD	521	20090925	A
	FBS	521	20091226	A
	FBS	521	20100210	A
	FBD	521	20100628	A
	FBS	521	20101229	A
	FBS	521	20110213	A
ASAR	IS2	19	20031126	D
	IS2	19	20040519	D
	IS2	19	20040728	D
	IS2	19	20041006	D
	IS2	19	20050119	D
	IS2	19	20050921	D
	IS2	19	20060104	D
	IS2	19	20060419	D
	IS2	19	20061220	D
	IS2	19	20070228	D
	IS2	19	20070509	D
	IS2	19	20090513	D
	IS2	19	20040623	D
SAR	IS2	19	19920503	D
	IS2	19	19920607	D
	IS2	19	19920816	D
	IS2	19	19920920	D
	IS2	19	19930314	D
	IS2	19	19960326	D
	IS2	19	19960327	D
	IS2	19	19960430	D
	IS2	19	19960501	D
	IS2	19	19980610	D
	IS2	19	19980922	D
	IS2	19	19980923	D

	IS2	19	19990317	D
	IS2	19	19990421	D
	IS2	19	19990526	D
	IS2	19	19990526	D
SAR	IS2	248	19920728	D
	IS2	248	19920901	D
	IS2	248	19921006	D
	IS2	248	19921110	D
	IS2	248	19921215	D
	IS2	248	19930119	D
	IS2	248	19930223	D
	IS2	248	19930330	D
	IS2	248	19930817	D
	IS2	248	19931026	D
	IS2	248	19931130	D
	IS2	248	19960411	D
	IS2	248	19960412	D
	IS2	248	19960516	D
	IS2	248	19960517	D
	IS2	248	19980904	D
	IS2	248	19990402	D
	IS2	248	19990507	D
	IS2	248	19990611	D

Table S2. List of offset-tracking pairs used in analysis

Sfraction is the fraction of the interval with summer days; Image pairs with S fraction larger than 60% were defined as summer, those with S fraction <40% i.e. with more than 60% winter days were defined as winter, and the remaining pairs were defined as equal summer-winter.

Sensor	ID of image pair	Date of image1	Date of image2	Interval days	Perpendicular baseline m	S fraction
ASAR track 177	261	20101109	20101209	30	8	0
	262	20101109	20110207	90	-156	0
	263	20101109	20110309	120	-381	0
	264	20101109	20110707	240	-754	40
	265	20101209	20110207	60	-165	0
	266	20101209	20110309	90	-390	0
	267	20101209	20110707	210	-763	45
	268	20110207	20110309	30	-225	0
	269	20110207	20110707	150	-598	64
	270	20110309	20110707	120	-374	80
PALSAR Track521	1	20070505	20070805	92	140	100
	2	20070505	20070920	138	-79	100
	3	20070505	20071105	184	569	80
	4	20070505	20080205	276	1074	53
	5	20070505	20080322	322	1047	46
	6	20070505	20080622	414	-265	55
	13	20070805	20070920	46	-219	100
	14	20070805	20071105	92	428	61
	15	20070805	20080205	184	934	30
	16	20070805	20080322	230	907	24
	17	20070805	20080622	322	-405	43
	24	20070920	20071105	46	647	23
	25	20070920	20080205	138	1152	7
	26	20070920	20080322	184	1125	5
	27	20070920	20080622	276	-187	33
	34	20071105	20080205	92	505	0
	35	20071105	20080322	138	478	0
	36	20071105	20080622	230	-834	35
	43	20080205	20080322	46	-27	0
	44	20080205	20080622	138	-1339	59
	51	20080322	20080622	92	-1313	89
	58	20080622	20090925	461	-426	60
	64	20090925	20091226	92	497	6
	65	20090925	20100210	138	988	4
	66	20090925	20100628	276	1334	33
	67	20090925	20101229	460	2123	40
	69	20091226	20100210	46	490	0
	70	20091226	20100628	184	836	47

Sensor	ID of image pair	Date of image1	Date of image2	Interval days	Perpendicular baseline m	S fraction
	71	20091226	20101229	368	1625	49
	72	20091226	20110213	414	2240	43
	73	20100210	20100628	138	346	63
	74	20100210	20101229	322	1135	56
	75	20100210	20110213	368	1750	49
	76	20100628	20101229	184	789	51
	77	20100628	20110213	230	1404	41
	78	20101229	20110213	46	614	0
ASAR track 19	183	20031126	20040519	175	226	27
	184	20031126	20040623	210	-73	39
	185	20031126	20040728	245	423	48
	186	20031126	20041006	315	360	57
	187	20031126	20050119	420	-17	43
	196	20040519	20040728	70	196	100
	197	20040519	20041006	140	134	95
	198	20040519	20050119	245	-244	54
	199	20040519	20050921	490	53	62
	207	20040623	20041006	105	432	93
	208	20040623	20050119	210	55	46
	209	20040623	20050921	455	352	59
	216	20040728	20041006	70	-63	90
	217	20040728	20050119	175	-440	36
	218	20040728	20050921	420	-144	56
	225	20041006	20050119	105	-378	0
	226	20041006	20050921	350	-81	49
	227	20041006	20060104	455	-178	39
	233	20050119	20050921	245	296	70
	234	20050119	20060104	350	199	51
	235	20050119	20060419	455	215	43
	240	20050921	20060104	105	-98	9
	241	20050921	20060419	210	-82	13
	242	20050921	20061220	455	-64	42
	246	20060104	20060419	105	15	16
	247	20060104	20061220	351	33	51
	248	20060104	20070228	421	97	43
	249	20060104	20070509	491	-111	44
	251	20060419	20061220	246	17	67
	252	20060419	20070228	315	81	52
	253	20060419	20070509	385	-127	52
	256	20061220	20070509	140	-145	26
	258	20070228	20070509	70	-209	53
SAR track 19	80	19920503	19920816	106	-380	100
	81	19920503	19920920	141	444	100
	82	19920503	19930314	316	152	47
	83	19920607	19920920	106	-244	100
	84	19920607	19930314	280	-537	40
	86	19920816	19930314	210	531	21

Sensor	ID of image pair	Date of image1	Date of image2	Interval days	Perpendicular baseline m	S fraction
	87	19920920	19930314	175	-293	5
	94	19960430	19980922	875	-456	58
	95	19960430	19980923	876	-790	58
	96	19960501	19980922	874	-352	58
	97	19960501	19980923	875	-686	58
	99	19980922	19990317	177	-196	5
	100	19980922	19990421	212	-70	13
	101	19980922	19990526	247	-59	25
	102	19980923	19990317	175	138	4
	103	19980923	19990421	210	264	13
	104	19980923	19990526	245	275	25
	106	19990317	19990526	70	136	77
SAR track248	109	19920728	19921006	70	277	90
	110	19920728	19921110	105	-147	60
	111	19920728	19921215	140	-363	45
	112	19920728	19930119	175	-364	36
	113	19920728	19930223	210	178	30
	114	19920728	19930330	245	9	26
	115	19920728	19930817	385	-534	52
	116	19920728	19931130	490	301	50
	118	19920901	19921110	70	-105	40
	119	19920901	19921215	105	-321	27
	120	19920901	19930119	140	-322	20
	121	19920901	19930223	175	220	16
	122	19920901	19930330	210	51	13
	123	19920901	19930817	350	-492	47
	124	19920901	19931130	455	343	46
	126	19921006	19921215	70	-641	0
	127	19921006	19930119	105	-641	0
	128	19921006	19930223	140	-99	0
	129	19921006	19930330	175	-268	0
	130	19921006	19930817	315	-811	43
	131	19921006	19931130	420	24	43
	133	19921110	19930119	70	-217	0
	134	19921110	19930223	105	325	0
	135	19921110	19930330	140	156	0
	136	19921110	19930817	280	-387	49
	137	19921110	19931130	385	448	47
	139	19921215	19930223	70	541	0
	140	19921215	19930330	105	372	0
	141	19921215	19930817	245	-171	56
	142	19921215	19931130	350	664	51
	144	19930119	19930330	70	373	0
	145	19930119	19930817	210	-170	65
	146	19930119	19931130	315	664	57
	148	19930223	19930817	175	-712	78
	149	19930223	19931130	280	122	64

Sensor	ID of image pair	Date of image1	Date of image2	Interval days	Perpendicular baseline m	S fraction
	150	19930330	19930817	140	-543	97
	151	19930330	19931130	245	291	73
	152	19930817	19931130	105	834	42
	157	19931130	19960411	863	-346	43
	158	19931130	19960412	864	-450	43
	159	19931130	19960516	898	-386	45
	160	19931130	19960517	899	-508	45
	164	19960411	19980904	876	-155	58
	167	19960412	19980904	875	-52	58
	170	19960516	19980904	841	-115	56
	173	19960517	19980904	840	7	56
	177	19980904	19990402	210	-410	13
	178	19980904	19990507	245	306	25
	179	19980904	19990611	280	-365	34
	181	19990402	19990611	70	44	100

Table S3: Details of window sizes shown in Figures S4-S8.

#	**Window name**	**No of Pixels range x azimuth**	**Km on ground East x North**
1	W0	80 x 400	595 x 1260
2	W1	64 x 320	476 x 1008
3	W2	48 x 240	357 x 756
4	W3	32 x 160	238 x 504
5	W4	24 x 120	178 x 378

FIGURES

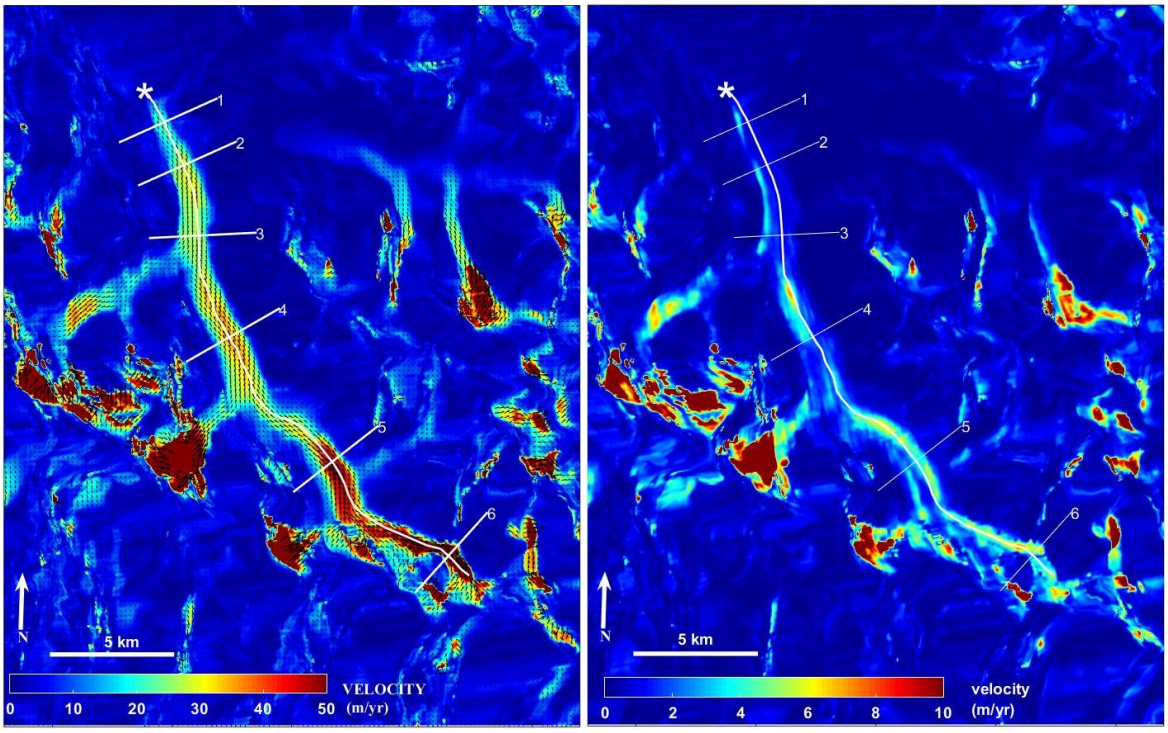

Figure S1. Winter surface velocity & velocity error map for the Gangotri Glacier.
This figure is identical to Figure 2 except that the color scale here is linear to facilitate comparison with the error map.

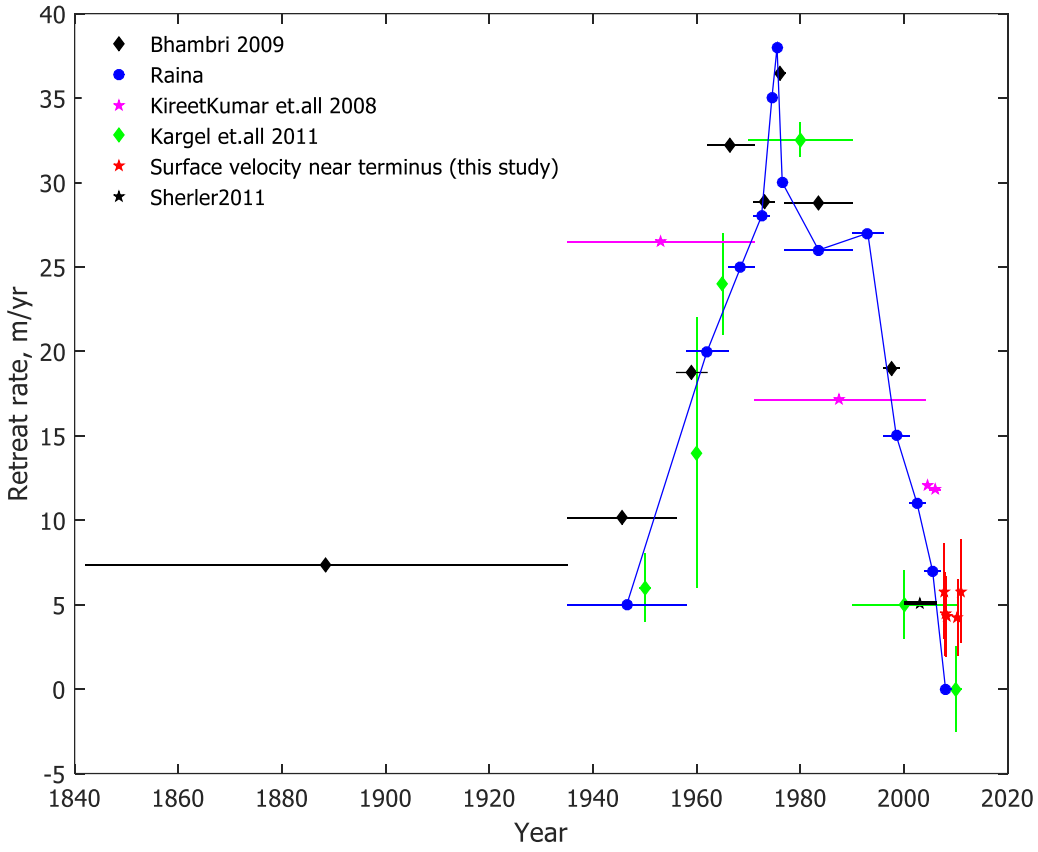

Figure S2. Comparison of surface velocity in this study with retreat rate observations. Retreat rates from different studies (references listed below) and terminus velocities within 0.5 km up-glacier from the terminus from this paper. See references for sources of retreat rate measurements used.

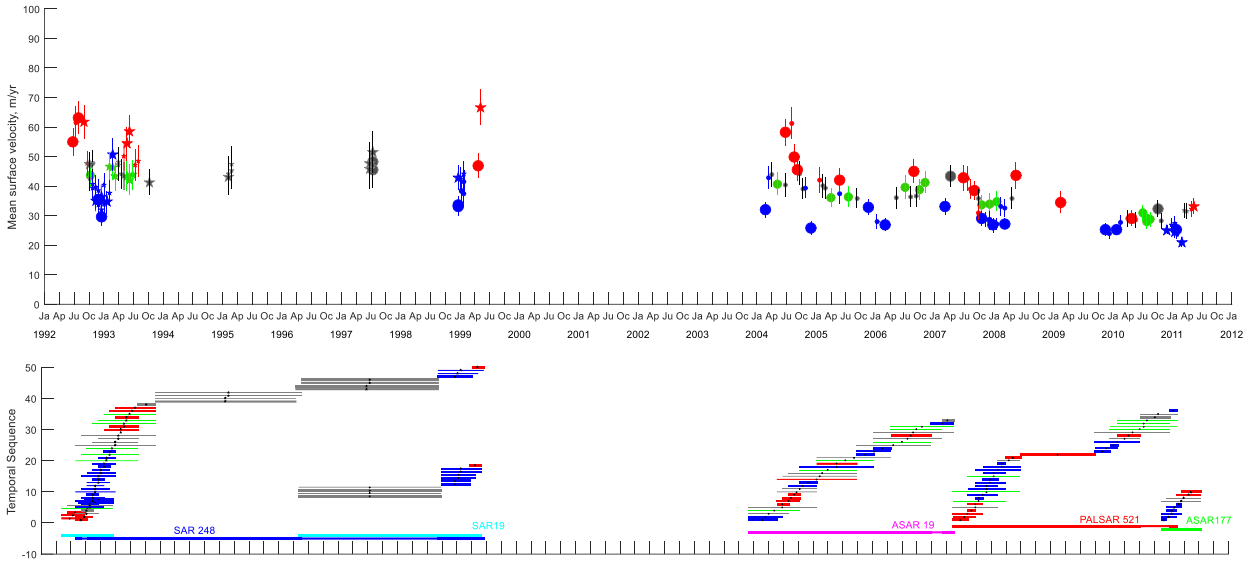

Figure S3: Temporal evolution of surface velocity for the Gangotri glacier for the complete range of available data (1992-2011). Conventions are as in Figure 6 & 7.
(A) Each point represents the mean surface velocity within the ablation region of the Gangotri glacier (0-12.6 km from the terminus) from one image pair with dates represented in (B) and mean standard deviation by error bars. Stars and circles represent data from satellites ERS248 and ERS19 respectively. Each line in (B) represents the start and end dates for image pairs matching the data in (A).

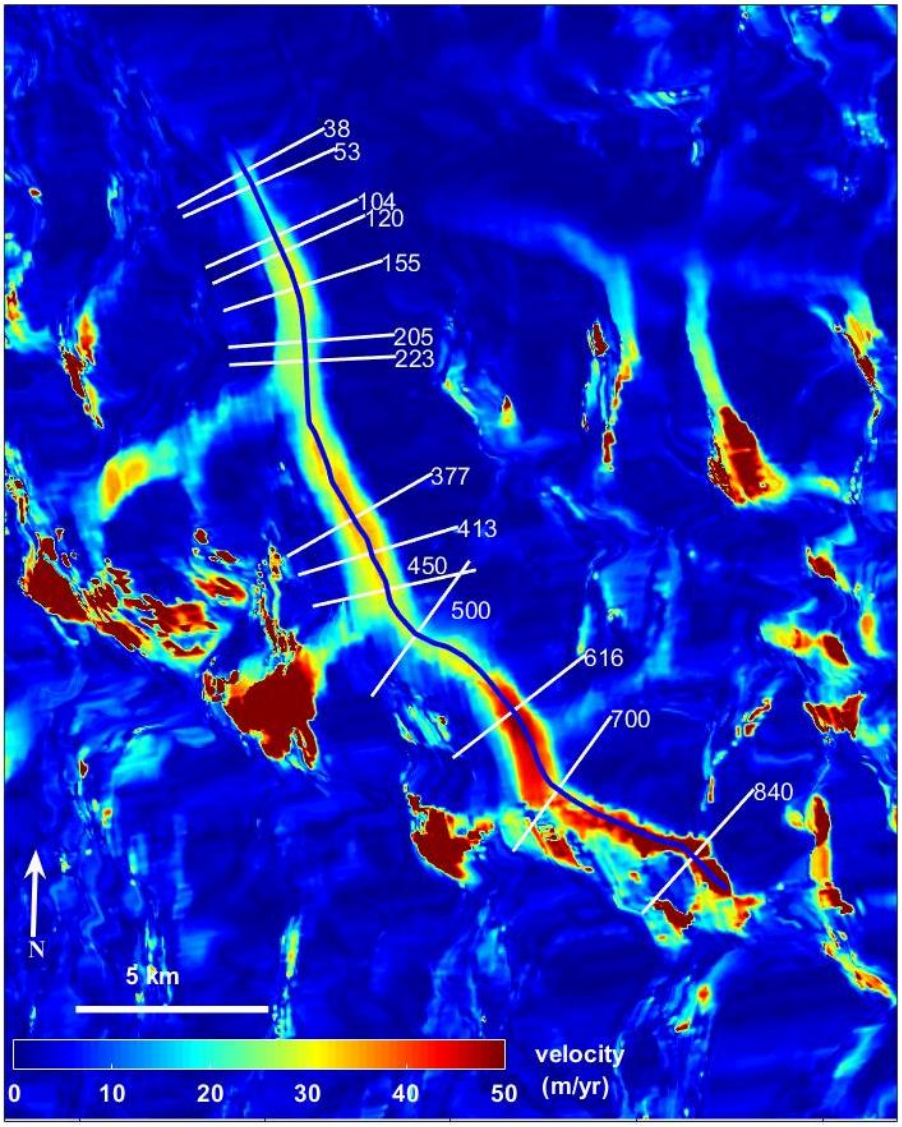

Figure S4: Surface velocity map for the Gangotri glacier showing the centerline of the glacier and across-profile locations for which velocities are shown in Figure S6. The image pairs used are the same as in Figure 1.

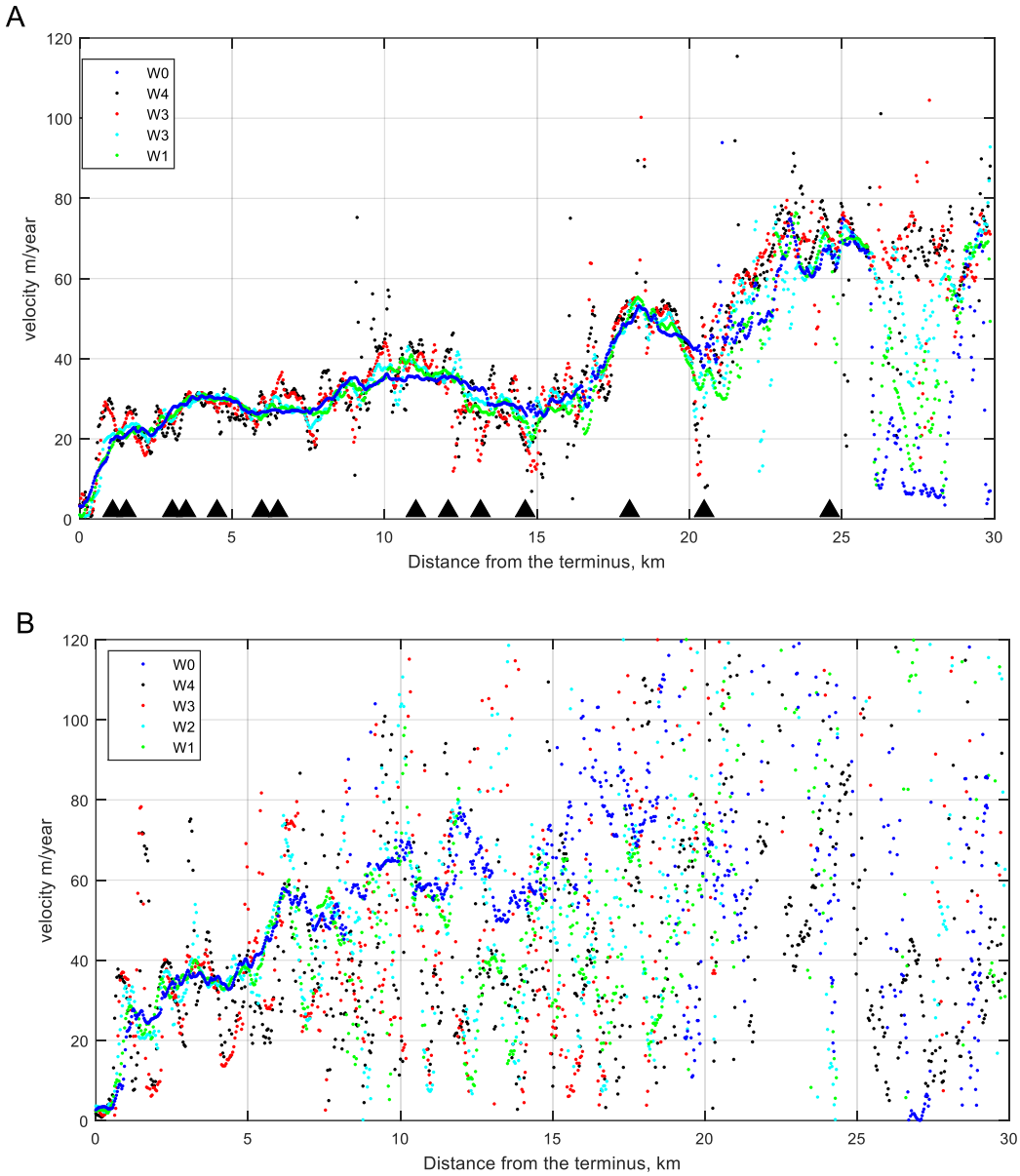

Figure S5: Effect of window size on winter and summer velocities along center line of the glacier.

(A) Winter pair: Image pair is the same as Figure S4. Plots show profiles of surface velocity in m/year for different window sizes listed in Table S3. Window W0, used in this paper, gives the best profile while the smaller windows give more noisy profiles. The black triangles on x-axis show locations of across profiles of velocity plotted in Figure S6.

(B**)** Summer pair:Data based on a summer image pair (5 May 2007-5 Aug 2007). Again, here window W0 gives the best result. Compared to winter, summer data is much more noisy and the velocities could be retrieved better within ~15-km up-glacier. Beyond this distance, velocity estimates are noisier.

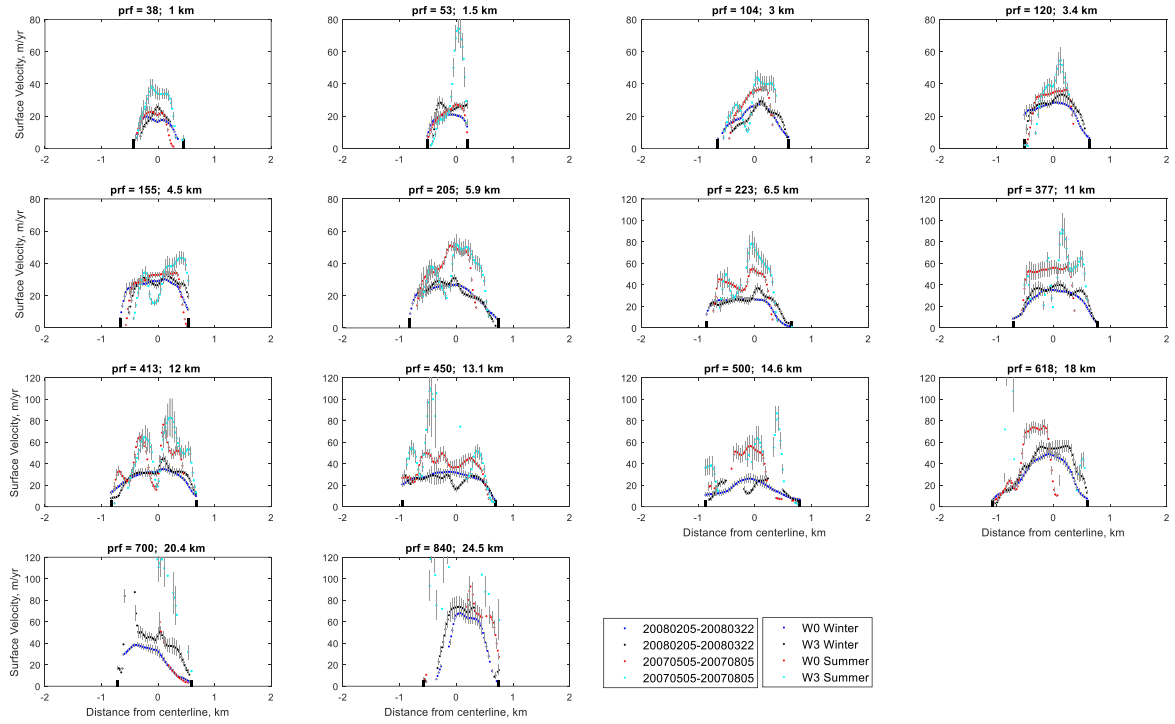

Figure S6. Effect of window size on winter and summer velocities across the glacier at various centerline locations shown in Figure S4.

Surface velocity profiles across the centerline of the glacier for 14 locations denoted by numbers (marked in Figure S4& Figure S5) are shown in each panel for the two window sizes (W0 and W3) for one summer period (image dates: 5 May 2007-5 Aug 2007) and one winter period (image dates: 5 Feb 2008-22 Mar 2008). It can be seen that the velocity estimated using large and small window size are similar in the winter but are truncated near the glacier margins (marked by thick vertical black lines for larger window sizes during summer. This is because when the glacier surface undergoes greater change in summer, the offset tracking method erroneously assigns zero velocities from the static regions outside the glacier to the regions inside the glacier. These artefactual velocities do not have a consistent direction of flow and are therefore rejected by the direction filter.